A publication of Phcog Net
Pharmacognosy Magazine
Home
Current issue
Instructions
Submit article

Pharmacogn Mag. 2015 May; 11(Suppl 1): S73–S85.
doi: 10.4103/0973-1296.157698: 10.4103/0973-1296.157698
PMCID: PMC4461972
PMID: 26109778

Anti-lung cancer potential of pure esteric-glycoside condurangogenin A against nonsmall-cell lung cancer cells *in vitro* via p21/p53 mediated cell cycle modulation and DNA damage-induced apoptosis

Sourav Sikdar, Avinaba Mukherjee, and Anisur Rahman Khuda-Bukhsh

Department of Zoology, Cytogenetics and Molecular Biology Laboratory, University of Kalyani, Kalyani, West Bengal, India

Address for correspondence: Prof. Anisur Rahman Khuda-Bukhsh, Department of Zoology, Cytogenetics and Molecular Biology Laboratory, University of Kalyani, Kalyani - 741 235, West Bengal, India. E-mail: prof_arkb@yahoo.co.in

Received 2014 Aug 8; Revised 2014 Sep 26; Accepted 2015 May 27.

Abstract

Background:

Marsdenia condurango (condurango) is a tropical woody vine native to South America. Our earlier study was limited to evaluation of anti-cancer potentials of crude condurango extract and its glycoside-rich components *in vitro* on lung cancer.

Objective:

This study aims at evaluating the effect of the single isolated active ingredient condurangogenin A (ConA; $C_{32}H_{42}O_7$) on A549, H522 and H460-nonsmall-cell lung cancer cells.

Materials and Methods:

ConA was isolated by column chromatography and analyzed by mass spectroscopy, Fourier transform infrared spectroscopy and proton-nuclear magnetic resonance. diphenyltetrazolium bromide assays were conducted on three cell-types using 6%-alcohol as control. Critical studies on cellular morphology, cell-cycle regulation, reactive oxygen species, mitochondrial membrane potential, and DNA-damage were made, and expressions of related signaling markers studied.

Results:

As IC_{50} doses of ConA proved to be too high and toxic to both A549 and H522 cells, all experimental studies were carried out on H460 cells with the IC_{50} dose (32 μg/ml − 24 h). Cellular morphology revealed typical apoptotic features after ConA treatment. At early treatment hours (2 h-12 h), maximum cells were arrested at G0/G1 phase that could be correlated with reduced level of cyclin D1-CDK with p21 up-regulation. At 18 h − 24 h, sub G0/G1 cell population was increased gradually, as revealed from cytochrome-c release and caspase-3 activation, further confirming the apoptosis-inducing ability of ConA at later phases. Gradual increase of TUNEL-positive cells with significant modulation of mitochondria-dependent apoptotic markers at longer time-points would establish apoptosis-induction property of ConA, indicating its potential as a strong candidate for anti-cancer drug formulation.

Conclusion:

Further studies are warranted against other types of cancer cells and animal models before its possible human use.

Keywords: Apoptosis, cell cycle, condurangogenin A, cyclin D1-CDK pathway, H460-nonsmall cell lung cancer cell, p21/p53

INTRODUCTION

There is increasing interest in investigating different plant species used as alternative medicines to identify effective ingredients using modern chemical and molecular methods.[1] Dried bark of condurango (*Marsdenia condurango*), belonging to Asclepiadaceae family is commonly used against a variety of digestive problems and esophageal cancer.[2,3,4]

Condurango glycosides (CGs), the biologically active component of condurango, have been reported to be a potent anti-tumor agent,[2] but the molecular mechanism of its anti-tumor activity remains unknown. In our earlier studies,[5,6] we reported the ability of crude ethanolic extract of condurango and of CG to induce cytotoxicity and apoptosis in several nonsmall-cell lung cancer (NSCLC) cell lines and in benzo[a] pyrene-induced lung cancer of rats. In this study, we report the anticancer potential of the isolated pure form of the major glycoside, namely, condurangogenin A ($C_{32}H_{42}O_7$, abbreviated henceforth as ConA) against lung cancer, which had not been studied earlier.

Lung cancer is one among the highest occurring cancers,[7] posing both economic and psychological challenges,[8] currently being the leading cause of cancer-related deaths in the United States and Western Europe.[9] NSCLC is more prevalent, accounting for 80% of all lung cancer cases.[10] Cigarette smoking is believed to be the primary cause of lung cancer and lung inflammatory diseases. Surgical resection is the only treatment for patients with Stage I or II NSCLC, whereas patients with later stages are often treated with combinations of surgery, chemotherapy, and radiation therapy.[11] Lung cancer hardly responds to conventional chemotherapy, primarily because of the mutation at KRAS, p53 like important regulator involved in normal tissue signaling, and often makes it resistant to chemotherapy.[12] Systematic drug delivery is rarely successful as only a limited amount of chemotherapeutic drugs can target lung tumor sites although they are administered at high doses; they often act on normal cells, inhibiting their growth.[13] In view of undesirable side-effects of both chemotherapies and radiation therapies, a search is on to find out some alternative agents and/or drugs that are equally effective, but have no or little side-effects. Thus, there is an urgent need to develop a promising chemotherapeutic agent, which has the potential to induce apoptosis-mediated cell death and has target specificity, having preferential destructive effects on cancer cells, but not on normal cells.

Since cell cycle regulation plays an important role during programmed cell death via p53/p21 or cyclin D1-CDK pathway, the major objectives of the present study were: (i) To chemically characterize pure form of ConA isolated from condurango extract; (ii) to evaluate its anticancer potential against NSCLC cells;

(iii) to ascertain if involvement of cell cycle regulators to promote programmed cell death was via reactive oxygen species (ROS)-generation and mitochondrial membrane potential (MMP)-depolarization; and (iv) to examine if ConA could induce apoptosis via DNA damage.

MATERIALS AND METHODS

Chemicals and reagents

Ethanolic bark extract of condurango was procured from Boiron Laboratory, Lyon, France. RPMI-1640, Fetal bovine serum (FBS), 0.05% trypsin-ethylenediaminetetraacetic acid (EDTA) were purchased from Gibco BRL (Grand Island, NY, USA). Antibiotic antimicotic solution was purchased from Himedia, India. Cell culture plastic wares were obtained from Tarsons (USA). All organic solvents used were of 99% (HPLC) High-performance liquid chromatography grade. Acridine orange/ethidium bromide (AO/EB), diphenyltetrazolium bromide (MTT), rhodamine123, diaminophenylindole (DAPI), H_2 DCFDA and all other chemicals used were purchased from Sigma Chemical Co.(St. Louis, MO, USA). All primary, secondary-HRP conjugated and secondary-FITC tagged antibodies were procured from Cell Signaling Technology, Inc., Beverly, Massachusetts.

Isolation of condurango-glycoside rich components of condurango

Mitsuhashi *et al.* (1984)[2] reported that ethanolic extract of condurango contains different types of glycosides, like CGs A, A_0, B, C, D, E_1, E_2, 20-O-methyl CG D, 20-iso-O-methyl CG D, Con A, C, E which have anti-tumor efficacy. Since the whole extract contained 65% alcohol (vehicle), alcohol content was first evaporated away at 45–50°C for 5–6 h from 500 ml of the original extract. The semi-dried extract was then kept under reduced pressure in a rotary evaporator to obtain a semisolid mass. After 2–3 days, a greenish mass was obtained, which contained the CG-rich component and weighed nearly 8.02 g. The semi-solid CG was then dissolved in 50 ml of 6% alcohol, stirred well and kept at 4°C for further use.

Molisch's test

It is a sensitive chemical test to detect the presence of carbohydrates, based on the dehydration of the carbohydrate by sulfuric acid to produce an aldehyde, which condenses with two molecules of phenol (usually α-naphthol, but also resorcinol, thymol) resulting in a red-or purple-colored compound. The test solution (CG) is combined with a small amount of Molisch's reagent (α-naphthol dissolved in ethanol) in a test tube. After mixing a small amount of concentrated sulfuric acid, it is slowly added down the sides of the sloping test-tube, without mixing, to form a bottom layer. A positive reaction is indicated by the appearance of a purple ring at the interface between the acid and test layers, indicating that the semisolid extract was positively glycoside-rich.[14]

Separation of pure esteric-glycoside from condurango glycosides by column chromatography

The dried CG was further separated by column chromatography to isolate specific and more purified single component of condurango if any, according to the method followed by Mitsuhashi *et al.* (1984).[2] *n*-hexane (nonpolar solvent), chloroform (nonpolar solvent) and methanol a (polar solvent)-mixture was used at 6:3:1 ratios. 10 fractions were collected with 50 ml each in 100 ml conical flasks. At a fraction, eight and nine, distinct single band was observed and confirmed by thin layer chromatography using the same solvent mixtures. These two fractions were selected for mass spectroscopy, proton nuclear magnetic resonance (1^H NMR) and Fourier transform infrared spectroscopy (FTIR) to know the molecular weight and structure (upto hydrogen number and functional group determination) of the isolated component.

Characterization of pure esteric glycoside

Mass spectroscopy of fraction nine revealed a distinct pick with a molecular weight of 538.29 which is similar to ConA. 1^H NMR data showed the presence of 42 hydrogen atoms and FTIR data confirmed the presence of pure esteric functional group, which is similar to ConA structure ($C_{32}H_{42}O_7$) [Figure 1].

Cell culture

A549, NCI-H522 (H522) and NCI-H460 (H460) human NSCLC cell lines were procured from NCCS, Pune, India. A549 cells were cultured in DMEM and H522 and H460 cells were cultured in RPMI-1640 medium supplemented with 10% heat inactivated FBS and 1% antibiotic antimicotic solution maintained at 37°C with 5% CO_2 in a humidified incubator. Cells were harvested with 0.05% trypsin-EDTA solution in phosphate buffer saline.

Determination of cell viability

Cell viability was determined by MTT assay. A549, H522 and H460 cells were dispensed in 96-well flat bottom microtiter plates at a density of 1×10^4 cells/well. After 48 h of incubation, cells were treated with various concentrations (30–45 μg/ml doses) of ConA for 12 h, 18 h, 24 h and 48 h, respectively, to determine the concentration of ConA at which the percentage of cell death was nearly 50%. Negative control cells received no drug that is, untreated (UT) and 6% alcohol (at which the ConA was dissolved) treated cells (6% Alc) were taken out for the experiment. The absorbance was measured at 595 nm (Mosmann, 1983) using an enzyme linked immunosorbent assay (ELISA) plate reader (Multiscan EX, Thermo Electron Corporation, USA). The relative percentage of viability was calculated.

Peripheral blood mononuclear cells analysis

Peripheral blood mononuclear cells (PBMC) was isolated from the blood sample of normal mice (99% homology with human) by conventional ficol gradient method and processed according to Biswas *et al.* (2011). The cells were treated with different concentrations of ConA and incubated for 24 h. The percentage of cell death was determined by MTT assay.[15]

Observation of morphological changes by light microscopy

Three types of NSCLC cells (A549, H522 and H460 cells) were plated in six-well culture plates (1×10^3 cells/well) and were treated with the IC_{50} dose against untreated and 6% Alc-treated controls. After 12 h, 18 h, 24 h and 48 h of ConA treatment, the cells were observed and photographed under inverted phase-contrast light microscope (Axiscope + 2, Zeiss, Germany).[5]

Flowcytometric analysis of cell cycle arrest by propidium iodide-staining

H460 Cells treated with ConA (IC_{50} dose) for different time-points (2 h, 6 h, 12 h, 18 h and 24 h) were used for ascertaining if there was cell cycle arrest at any particular stage by propidium iodide (PI) (50 μg/ml) staining-flowcytometric analysis.[16] Cell-cycle histograms were generated after analysis of PI-stained cells by fluorescence-activated cell sorting (FACS) Aria III (BD Bioscience, Germany) to determine the percentage of cells in each phase (sub G1, G0/G1, S, and G2/M).

Determination of reactive oxygen species accumulation

Reactive oxygen species generation being an early event of apoptosis, H460 cells were treated with IC_{50} dose of ConA for different periods of time (2 h, 6 h, 12 h, 18 h and 24 h) and incubated with 2', 7'-dichlorodihydrofluoresceindiacetate (H_2 DCFDA) (20 μM) for 15 min. Then the potential of ConA to generate oxidative stress in terms of intracellular H_2O_2 was quantitatively analyzed by fluorimeter (PerkinElmer) and photographed under fluorescence microscope.[17]

Changes in mitochondrial membrane potential

The changes in MMP after ConA treatment were observed by a fluorescent probe, rhodamine 123. As change in MMP is also an early event of apoptosis like ROS accumulation, the changes in the MMP of cells were observed at different time points (2 h, 6 h, 12 h, 18 h and 24 h) by fluorescence microscope (Axioscope plus 2, Zeiss) and flowcytometry (FACS Aria III, BD Bioscience).[18]

Changes in nuclear morphology

H460 cells after ConA treatment for 12 h, 18 h and 24 h were stained with DAPI (10 μg/ml), observed under fluorescence microscope (Axiscope + 2, Zeiss, Germany) and representative photographs were taken.[19] ConA treated and untreated cells were observed and photographed under a fluorescence microscope (Axiscope plus 2, Zeiss, Germany) after AO/EB staining to determine DNA-nick generation. [20]

DNA fragmentation assay

After the treatment with different concentrations of ConA for 12 h, 18 h and 24 h, DNA was extracted using conventional phenol/chloroform method. Finally, DNA was separated in 2% agarose gel containing EB and visualized under ultra violet transilluminator.[5]

Deoxyuridine triphosphate-nick generation by TUNEL assay

DNA strand breakage was also analyzed by labeling the treated and untreated H460 cells with bromolated-deoxyuridine triphosphate (Br-dUTP) following the method of Darzynkiewicz *et al.* (2008)[21] at 12 h, 18 h and 24 h time-points. DNA-end labeling was performed using the BD FACS Verse™ system, and the data analyzed using the BD FACS Suite™ software (BD Bioscience, São Paulo). For each sample 10,000 cells were counted.

Semi-quantitative reverse transcriptase polymerase chain reaction

Total RNA was extracted from the experimental cells using Trizol reagent according to the manufacturer's instructions and cDNA preparation and amplification were done at 12 h, 18 h and 24 h time-points according to the method of Chowdhury *et al.* (2008).[22] Band-intensities were measured by using ("Image J" Software, Germany, version 1.45). The oligonucleotide (primer) sequences are mentioned in Table 1. Major apoptosis markers like Bax, Bcl_2, cytochrome-c and caspase-3 were analyzed. GAPDH served as the house-keeping gene.

Indirect-enzyme linked immunosorbent assay

The protein activities of major apoptosis markers (Bax, Bcl_2, cytochrome-c and caspase-3) and cell cycle markers (cyclin D1, CDK2, p21 and p53) were measured by using an ELISA reader at 12 h, 18 h and 24 h time-points of treatment against UT. GAPDH served as the house-keeping gene. The color intensity was measured at 405 nm with respect to blank.

Western blot

For western blot analyses equal amount of protein was loaded and samples were denatured in 12% sodium dodecyl sulfate–polyacrylamide gel electrophoresis and were transferred separately onto PVDF membranes. Anti-Bax, Bcl_2, cytochrome-c, caspase-3, poly ADP-ribose polymerase (PARP), cyclin D1, CDK2, p21 and p53 primary antibodies (1:1000) were used for this study along with HRP-conjugated secondary antibodies (1:2000) and were developed by DAB-H_2 O_2 system. Quantification of proteins was done by densitometric analysis using Image J Software.[7]

Blinding

The observers were blinded during observation as to whether they were observing the control and/or drug-treated materials.

RESULTS

Analysis of cell viability and selection of drug doses

Results of MTT assay at 12 h, 18 h, 24 h and 48 h, respectively, with 30–45 μg/ml doses of ConA revealed that IC_{50} doses of ConA on A549 and H522 cells 38 μg/ml and 39 μg/ml, respectively for 24 h) were too high [Figure 2]. But 32 μg/ml dose (IC_{50} dose) for 24 h treatment on H460 cells had the capacity to destroy nearly 50% of cells and this dose was therefore selected for all the experimental schedules to test whether ConA could produce possible anti-cancer effect against H460 in a time-and dose-dependent manner. Suitable 6% alcohol control was also maintained, which had no cytotoxic effect on H460 at its highest dose used (0.4 μl/ml) for both 12 h and 24 h fixation intervals. The cytotoxicity of 32 μg/ml of ConA was also checked for PBMC which showed a minimal effect [Figure 3].

Morphological changes of A549, H522 and H460 cells by light microscopy

A critical study of cell morphologies provided preliminary indication of the cell-death inducing potential of respective IC_{50} doses of ConA on different NSCLC cell lines at different hour intervals (12 h, 18 h, 24 h and 48 h). Results showed that there were no significant changes in morphologies of A549 and H522 cells at different time-points [Figure 2]. On the other hand, treatment with 32 μg/ml dose of ConA on H460 cells showed that at 12 h and 18 h of ConA treatment, cells shrunk with reduction in cell-size and number against untreated and 6% alcohol-treated cells. But at 24 h of treatment, the cells became very much reduced in size with a rounded shape and the cell number was reduced to nearly 50% [Figure 4]. At 48 h of ConA treatment, all the cells became dead, for which this time-point was not considered for further experiments. Therefore, the study on A549 and H522 was not further extended. As the cell morphologies of 6% alcohol treated cells at 12 h, 18 h and 24 h time-points were nearly similar with untreated cells, alcohol control was not considered for further experiments.

Cell cycle analysis

To study the mode of cell death induced by ConA, flow cytometric analysis was performed with 32 μg/ml dose at different hour intervals against untreated cells. Incubation of fixed and permeabilized cells with PI results in quantitative PI-binding with total cellular DNA and the fluorescence intensity of PI-labeled cells was proportional to DNA contents.

At early hour intervals of ConA treatment (2 h, 6 h and 12 h) with 32 μg/ml dose, maximum cells were arrested at G0/G1 phase with the increase of time-points, which would suggest that ConA had an interfering ability on the DNA replication by prolonged G0/G1 arrest and also suggested that it inhibited the cells to go forward in the S phase. But for the long term treatment (18 h and 24 h), sub G0/G1 cell population was certainly increased gradually with the decrease of G0/G1; this would further indicate the presence and increase of sub-diploid cell population which may trigger apoptosis for long term effect of ConA treatment with respect to untreated and ConA-treated cells at early hours [Figure 5].

Estimation of accumulated reactive oxygen species

Fluorescence microscopy and fluorimetric study revealed that at 12 h time-point of ConA treatment, maximum ROS was generated against untreated cells [Figure 6].

Analysis of mitochondrial membrane potential depolarization

Fluorescence microscopic study revealed that at 18 h time-point, the MMP depolarization was at maximum, which was also supported by the analysis of flowcytometric data [Figure 7].

Study on chromatin condensation by diaminophenylindole and acridine orange/ethidium bromide staining

Results revealed that at 12 h time-point, DAPI fluorescence intensity was not so much prominent presumably because the cells were not prepared to enter into the subG0/G1 phase, rather they were at G0/G1 phase in increased amount as evidenced by cell cycle analysis. But at 18 h and 24 h of ConA treatment, the fluorescent intensity of DAPI was gradually increased against untreated cells (indicated by arrows). Interestingly, at 24 h time-point, more DAPI fluorescence was observed that may prove that at 24 h of ConA treatment, maximum DNA-nick generation occurred, a phenomenon that is known to be associated with the apoptosis generation at the late phase of treatment.

Further, AO/EB staining revealed that at 12 h time-point the AO/EB fluorescence intensity was not markedly changed. But at 18 h and 24 h of ConA treatment, cells completely took the red fluorescence of EB, which may suggest that the maximum cell death occurred at the late phase of ConA treatment via chromatin condensation or DNA breakage, as compared to untreated cells, and would testify that the cells.

DNA fragmentation

Apoptosis was marked by the formation of fragmented DNA, which was further confirmed by DNA fragmentation assay [Figure 8c]. Result distinctly showed the formation of DNA laddering at 18 h and 24 h of ConA treatment, but not at 12 h of treatment in respect to untreated DNA. The DNA laddering was much more prominent at 24 h of treatment specifically suggesting that at this time-point the ConA had the maximum capacity to induce apoptosis via DNA breakage; this was also supported by DAPI, AO/EB staining and TUNEL assay results.

Deoxyuridine triphosphate-nick generation by TUNEL assay

DNA strand breakage was further analyzed by Br-dUTP nick end-labeling (TUNEL assay) at different hour intervals (12 h, 18 h and 24 h) of ConA treatment against untreated cells. Results of TUNEL assay revealed the gradual increase of dUTP-nick by forming TUNEL-positive nuclei in ConA-treated cells with the increase of time of treatment with respect to untreated cells, quantitatively [Figure 8c]. Maximum TUNEL-positive cells were obtained at 24 h of treatment which further suggests that the DNA strand breakage occurred at the late phase of treatment that might have triggered apoptosis.

Study on expressions of cell cycle markers at protein level

The cell cycle analysis has previously showed the increase of cells at G0/G1 level, at early phases of ConA treatment (2 h, 6 h and 12 h) with 32 μg/ml dose, but at the late phases (18 h and 24 h) the cells were arrested to the maximum at sub G0/G1. So for further verification, the expressions of cell cycle markers like cyclin D1, CDK2, p21, p53 were analyzed at protein level by ELISA and western blot.

Results of ELISA and western blot revealed significant downregulation of cyclin D1-CDK2 with p21 and p53 up-regulation in the early phases of treatment, specifically at 12 h against untreated samples. But in the late phases of treatment, downregulation of cyclin D1-CDK1 and p21 was found with the increased expression of p53 [Figure 9].

Study on apoptosis markers at mRNA and protein levels

The expressions of major apoptosis markers involved in the mitochondria-dependent intrinsic pathway of apoptosis were evaluated at mRNA and protein levels at 12 h, 18 h and 24 h intervals as apoptosis induction was mainly observed at the late phases of treatment, especially at 18 h and 24 h intervals. The

results of reverse transcriptase polymerase chain reaction, ELISA and western blot analysis of Bax/Bcl_2 revealed significant upregulation of Bax and downregulation of Bcl_2 at 12 h of treatment against untreated samples. Further the expression of cytochrome-c was evaluated as the MMP depolarization occurred at the 18 h of treatment. The results of cytochrome-c expression at both mRNA and protein levels revealed that at 18 h of treatment cytochrome-c expression was at the maximum as compared to the untreated control. For further confirmation of caspase-3 mediated apoptosis generation after cytochrome-c release, the expression of caspase-3 was also observed at both mRNA and protein levels. Results showed a significant increase of expression of caspase-3 at 24 h interval which might stimulate the cleavage of PARP. The western blot analysis of PARP at different hour intervals showed that at 24 h time-point, PARP cleavage occurred by the formation of active 89 kDa and inactive 116 kDa subunits where band-intensity was significantly increased in 89 kDa fragment against untreated controls [Figure 10]. This result would suggest the apoptosis induction property of ConA at the late phases [Figure 11].

DISCUSSION

Condurangogenin A was previously isolated by Mitsuhashi *et al.* (1984) for the first time and subsequently by Berger *et al.* (1988),[3] but the anticancer potential had not been ascertained earlier. Six pregnane-glycosides have so far been isolated from condurango bark of which CGs A and C are reported to be most effective ingredients.[2] Structural derivatives of some other glycosidic components like Con A, C and E have also been reported,[3] but their anti-cancer activity has not been established.

Since many phytochemicals such as, flavones, glycosides, catechins, etc., isolated from different herbs or plant extracts have already been researched and found to be useful remedies against cancer, we became interested to study if ConA isolated in its pure form could also have anticancer potential against lung cancer, for which proper drug for treatment is still in search. Results of cell viability at 12 h, 18 h, 24 h and 48 h, respectively, with 30-45 μg/ml doses of ConA revealed that IC_{50} doses of ConA on A549 and H522 cells (38 μg/ml and 39 μg/ml, respectively for 24 h) were too high. For further confirmation, the cellular morphologies of ConA-treated A549 and H522 cells were further evaluated by LM against untreated controls at different time-points. Results showed absence of apoptotic changes in A549 and H522 cells, for which we did not further continue the study on the two cell lines, A549 and H522 cells.

Results of H460 cell viability showed that 32 μg/ml (the IC_{50} value) of ConA for 24 h was able to annihilate quite a large number of cancer cells which normally are known to fend off stubbornly all apoptotic signals. Positive features typical of apoptosis, such as cellular morphology, FACS data, etc., confirmed the efficacy of ConA in inducing cell death in the cancer cells. FACS data of cell cycle regulation further revealed that at early treatment hours (2 h, 6 h and 12 h) with the IC_{50} dose, maximum number of cells was arrested at G0/G1 phase. But for the long term treatment (18 h and 24 h), G0/G1 cell population was certainly reduced with the increase of sub G0/G1 cell population.

There are many anticancer formulations in ancient and modern medicinal books, which should provide a guide along with clinical evidences for the identification of new anti-cancer compounds.[23] In recent years, many cancer patients are now being treated with complementary/alternative medicines as supportive care for their less toxic side-effects.[24] Thus traditional medicinal plant extracts and their active components have re-ignited research for ascertaining and evaluating their scientific roles in cancer treatment and successfully gained medical, economic and sociological importance.[25]

Human cancer cells are known to deactivate the p53-p21 pathway to induce activities in the cell cycle markers like CDK4, CDK2, cyclin D1 needed for continual DNA synthesis. On the contrary, induced p21 binds to the cyclin D1/CDK2 complexes and inhibits their kinase activities. Results of ELISA and western blot revealed significant downregulation of cyclin D1-CDK2 with p21 and p53 up-regulation in the early phases of treatment, specifically at 12 h of treatment against untreated samples. This finding could establish that activation of the p53-p21 pathway is responsible for the ConA-induced G0/G1-phase

checkpoint response at early phases of treatment. This provides the first evidence for p21 induction by p53 during DNA damage-induced G0/G1-phase that inhibits both cyclin D1 and CDK2 activities at the same phase of treatment. But at the later phases of treatment, downregulation of cyclin D1-CDK2 and p21 expression with increased expression of p53 suggest that cells undergo DNA damage-induced apoptosis due to nonfunctional activity of cyclin D1-CDK2 and p21 at this stage. But as p53 is a tumor suppressor gene and also involved in the DNA damage induced apoptosis, so the expression level was gradually increased at the late phases of ConA treatment also.

ConA also has ROS accumulation capacity at an early hour (12 h) of treatment which mediates MMP depolarization at 18 h time-point. Moreover, gradual increase of fluorescence intensity of DAPI and AO/EB with increased TUNEL-positive cell population and DNA fragmentation at 18 h and 24 h of ConA treatment gave a positive hint towards apoptosis generation by affecting DNA at the late hours. Significant up-regulation and down-regulation of mitochondria-dependent pro-apoptotic gene (Bax, cytochrome-c, caspase-3) and anti-apoptotic gene (Bcl_2), respectively, with the increase of time-points, especially at 18 h and 24 h of ConA treatment would support the apoptosis induction property of ConA at the late phase of treatments.

CONCLUSION

This study clearly suggests the anticancer potential of ConA against NSCLC cells via cell cycle modulation and apoptosis generation, which needs a preclinical trial in carcinogen-induced lung cancer in animal models to determine if it can be recommended for use for human lung cancer treatment, at least as a supportive medicine.

ACKNOWLEDGMENT

This work was financially supported by a grant to Prof. A.R. Khuda-Bukhsh, Department of Zoology, University of Kalyani by Boiron Laboratory, Lyon, France. The authors are very much thankful to Chemistry Department, University of Kalyani, West Bengal, India, for help during FTIR and ^{13}C NMR and Dr. Sanjaya Mallick, Application Scientist, University of Calcutta, for his guidance during FACS. The authors are also very much grateful to IICB, Kolkata, West Bengal, India for help during mass spectroscopy.

Footnotes

Source of Support: This work was financially supported by a grant to Prof. A.R. Khuda-Bukhsh, Department of Zoology, University of Kalyani by Boiron Laboratory, Lyon, France. The authors are very much thankful to Chemistry Department, University of Kalyani, West Bengal, India, for help during FTIR and 13C NMR and Dr. Sanjaya Mallick, Application Scientist, University of Calcutta, for his guidance during FACS

Conflict of Interest: None declared.

REFERENCES

1. Wang X, Zhang F, Yang L, Mei Y, Long H, Zhang X, et al. Ursolic acid inhibits proliferation and induces apoptosis of cancer cells *in vitro* and *in vivo*. J Biomed Biotechnol. 2011;2011:419343. [PMCID: PMC3116524] [PubMed: 21716649]

2. Mitsuhashi H, Shigeru A, Koji H, Hiroshi M, Den-Ich M, Toshiharu N, et al. Condurango glycoside compounds, processes for their preparation, antitumor agents comprising them and compositions. United States Patent. 1984:1–11.

3. Berger S, Junior P, Kopanski L. Structural revision of pregnane ester glycosides from condurango cortex and new compounds. Phytochemistry. 1988;27:1451–8.

4. Banerji P, Campbell DR, Banerji P. Cancer patients treated with the Banerji protocols utilising homoeopathic medicine: A Best Case Series Program of the National Cancer Institute USA. Oncol Rep. 2008;20:69–74. [PubMed: 18575720]

5. Sikdar S, Mukherjee A, Boujedaini N, Khuda-Bukhsh AR. Ethanolic extract of condurango (*Marsdenia condurango*) used in traditional systems of medicine including homeopathy against cancer can induce DNA damage and apoptosis in nonsmall lung cancer cells, A549 and H522, *in vitro*. TANG Int J Genuine Tradit Med. 2013;3:1–10.

6. Sikdar S, Mukherjee A, Ghosh S, Khuda-Bukhsh AR. Condurango glycoside-rich components stimulate DNA damage-induced cell cycle arrest and ROS-mediated caspase-3 dependent apoptosis through inhibition of cell-proliferation in lung cancer, *in vitro* and *in vivo*. Environ Toxicol Pharmacol. 2014;37:300–14. [PubMed: 24384279]

7. Hsu HF, Huang KH, Lu KJ, Chiou SJ, Yen JH, Chang CC, et al. Typhonium blumei extract inhibits proliferation of human lung adenocarcinoma A549 cells via induction of cell cycle arrest and apoptosis. J Ethnopharmacol. 2011;135:492–500. [PubMed: 21470575]

8. Arora R. New Delhi, India: Jaypee Brothers Medical Publishers (P) Ltd; 2010. Herbal Medicine: A Cancer Chemopreventive and Therapeutic Perspective.

9. Ji BC, Hsu WH, Yang JS, Hsia TC, Lu CC, Chiang JH, et al. Gallic acid induces apoptosis via caspase-3 and mitochondrion-dependent pathways *in vitro* and suppresses lung xenograft tumor growth *in vivo*. J Agric Food Chem. 2009;57:7596–604. [PubMed: 20349925]

10. Bishop JA, Benjamin H, Cholakh H, Chajut A, Clark DP, Westra WH. Accurate classification of non-small cell lung carcinoma using a novel microRNA-based approach. Clin Cancer Res. 2010;16:610–9. [PubMed: 20068099]

11. Tseng CL, Wu SY, Wang WH, Peng CL, Lin FH, Lin CC, et al. Targeting efficiency and biodistribution of biotinylated-EGF-conjugated gelatin nanoparticles administered via aerosol delivery in nude mice with lung cancer. Biomaterials. 2008;29:3014–22. [PubMed: 18436301]

12. Guo W, Wu S, Liu J, Fang B. Identification of a small molecule with synthetic lethality for K-ras and protein kinase C iota. Cancer Res. 2008;68:7403–8. [PMCID: PMC2678915] [PubMed: 18794128]

13. Taraphdar AK, Roy M, Bhattacharya RK. Natural products as inducers of apoptosis: Implication for cancer therapy and prevention. Curr Sci. 2001;80:1387–96.

14. Glycosides; Glycosides. Available from: http://www.en.wikipedia.org/wiki/Glycoside. http://www.uomustansiriyah.edu.iq/008/phar/readpdf.php?id=5 .

15. Mosmann T. Rapid colorimetric assay for cellular growth and survival: Application to proliferation and cytotoxicity assays. J Immunol Methods. 1983;65:55–63. [PubMed: 6606682]

16. Gao N, Flynn DC, Zhang Z, Zhong XS, Walker V, Liu KJ, et al. G1 cell cycle progression and the expression of G1 cyclins are regulated by PI3K/AKT/mTOR/p70S6K1 signaling in human ovarian cancer cells. Am J Physiol Cell Physiol. 2004;287:C281–91. [PubMed: 15028555]

17. Bishayee K, Paul A, Ghosh S, Sikdar S, Mukherjee A, Biswas R, et al. Condurango-glycoside-A fraction of *Gonolobus condurango* induces DNA damage associated senescence and apoptosis via ROS-dependent p53 signalling pathway in HeLa cells. Mol Cell Biochem. 2013;382:173–83. [PubMed: 23807740]

18. Ling YH, Liebes L, Zou Y, Perez-Soler R. Reactive oxygen species generation and mitochondrial dysfunction in the apoptotic response to Bortezomib, a novel proteasome inhibitor, in human H460 non-small cell lung cancer cells. J Biol Chem. 2003;278:33714–23. [PubMed: 12821677]

19. Biswas R, Mandal SK, Dutta S, Bhattacharyya SS, Boujedaini N, Khuda-Bukhsh AR. Thujone-rich fraction of *Thuja occidentalis* demonstrates major anti-cancer potentials: Evidences from *In Vitro* studies on A375 cells. Evid Based Complement Alternat Med. 2011;2011:568148. [PMCID: PMC3106972] [PubMed: 21647317]

20. Chen Y, McMillan-Ward E, Kong J, Israels SJ, Gibson SB. Mitochondrial electron-transport-chain inhibitors of complexes I and II induce autophagic cell death mediated by reactive oxygen species. J Cell Sci. 2007;120:4155–66. [PubMed: 18032788]

21. Darzynkiewicz Z, Galkowski D, Zhao H. Analysis of apoptosis by cytometry using TUNEL assay. Methods. 2008;44:250–4. [PMCID: PMC2295206] [PubMed: 18314056]

22. Chowdhury R, Dutta A, Chaudhuri SR, Sharma N, Giri AK, Chaudhuri K. *In vitro* and *in vivo* reduction of sodium arsenite induced toxicity by aqueous garlic extract. Food Chem Toxicol. 2008;46:740–51. [PubMed: 17983699]

23. Cheng YL, Lee SC, Lin SZ, Chang WL, Chen YL, Tsai NM, et al. Anti-proliferative activity of *Bupleurum* scrozonerifolium in A549 human lung cancer cells *in vitro* and *in vivo*. Cancer Lett. 2005;222:183–93. [PubMed: 15863267]

24. Rostock M, Naumann J, Guethlin C, Guenther L, Bartsch HH, Walach H. Classical homeopathy in the treatment of cancer patients – A prospective observational study of two independent cohorts. BMC Cancer. 2011;11:19. [PMCID: PMC3035587] [PubMed: 21241504]

25. Saini A, Berruti A, Capogna S, Negro M, Sguazzotti E, Picci RL, et al. Prevalence of complementary/alternative medicines (CAMs) in a cancer population in northern Italy receiving antineoplastic treatments and relationship with quality of life and psychometric features. Qual Life Res. 2011;20:683–90. [PubMed: 21080084]

Figures and Tables

Figure 1

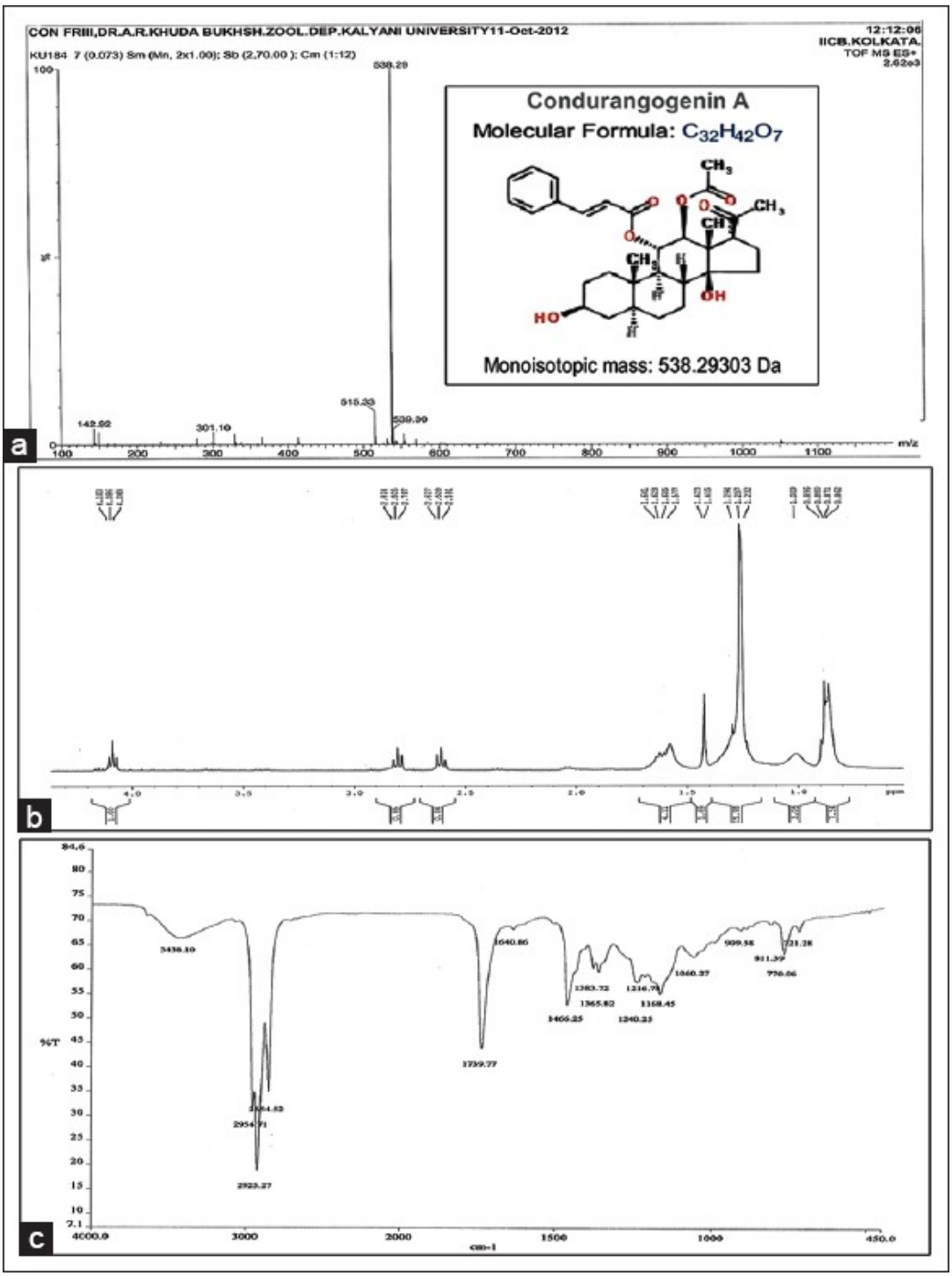

Open in a separate window

(a) Mass spectroscopy of condurangogenin A (ConA), molecular weight (monoisotopic mass) of 538.29. (b) Proton nuclear magnetic resonance of ConA showed the presence of 42 hydrogen atoms. (c) Fourier transform infrared spectroscopy of ConA

Table 1

Primer sequences

Primer	Primer sequences
Bax	Fwd 5'-AGTAACATGGAGCTGCAGAGG-3' Rev 5'-ATGGTTCTGATCAGTTCCGG-3'
Bcl_2	Fwd 5'-GTGACTTCCGATCAGGAAGG-3' Rev 5'-CTTCCAGACATTCGGAGACC-3'
Caspase-3	Fwd 5'-AGGGGTCATTTATGGGACA-3' Rev 5'-TACACGGGATCTGTTTCTTTG-3'
Cytochrome-c	Fwd 5'-CGTGTCGACCTAATATGGGTGAT GTTGAAAAGG-3' Rev 5'-ACAGATCTTTCTCATTAGTAGCC TTTTTAAG-3'
GAPDH	Fwd 5'-CCATGTTCGTCATGGGTGTGAACCA-3' Rev 5'-GCCAGTAGAGGCAGGGATGATGTTC-3'

GAPDH: Glyceraldehyde-3-phosphate dehydrogenase

Figure 2

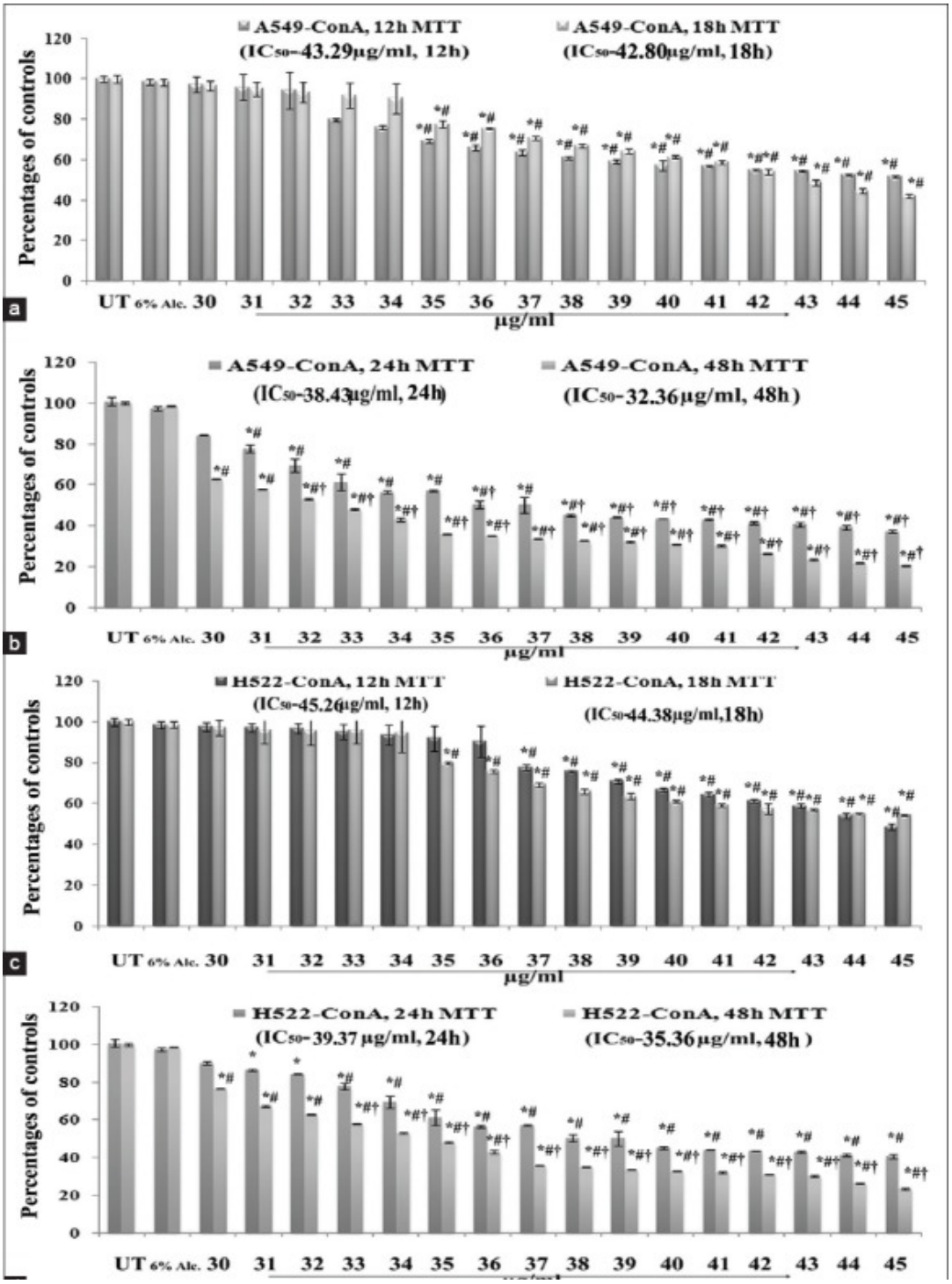

Open in a separate window

Effect of condurangogenin A (ConA) on the viability of A549 and H522 cells A549 cells were exposed to ConA for 12 h, 18 h and (b) exposed to ConA for 24 h and 48 h, respectively, at different concentrations (30-45 µg/ml) and the cell viability was determined by diphenyltetrazolium bromide (MTT) assay. Results were expressed as percentage of cell viability and each expressed as mean ± standard division (SD) ($N = 6$). Significance, *$P < 0.05$ versus untreated (UT) and #$P < 0.05$ versus 6% Alc-treated groups. Significance, $P < 0.001$ versus UT. (c) H522 cells were exposed to ConA for 12 h, 18 h and (d) exposed to ConA for 24 h and 48 h, respectively, at different concentrations (30–45 µg/ml) and the cell viability was determined by MTT assay. Results were expressed as percentage of cell viability and each expressed as mean ± SD ($N = 6$). Significance, *$P < 0.05$ versus untreated (UT) and #$P < 0.05$ versus 6% Alc.-treated groups. Significance, †$P < 0.001$ versus UT

Figure 3

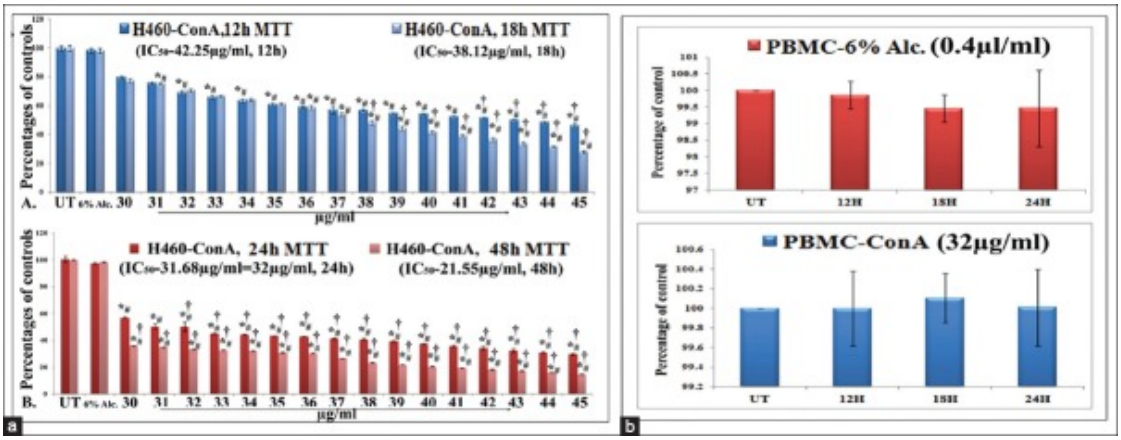

(a) Effect of condurangogenin A (ConA) on the viability of H460 cells. Cells were exposed to ConA for 12 h, 18 h, 24 h and 48 h, at different concentrations (30–45 µg/ml) and the cell viability was determined by diphenyltetrazolium bromide (MTT) assay. 6% alcohol (6% Alc.) was used as vehicle control. Results were expressed as percentage of cell viability and each expressed as mean ± standard division ($N = 6$). Significance, *$P < 0.05$ versus untreated (UT) and #$P < 0.05$ versus 6% Alc.-treated groups. Significance, $P < 0.001$ versus UT. (b) Effect of 6% Alc. (0.4 µl/ml) and ConA (32 µg/ml) on peripheral blood mononuclear cells (PBMC) by MTT assay. PBMCs were incubated for 12 h, 18 h and 24 h with 6% Alc. and ConA

Figure 4

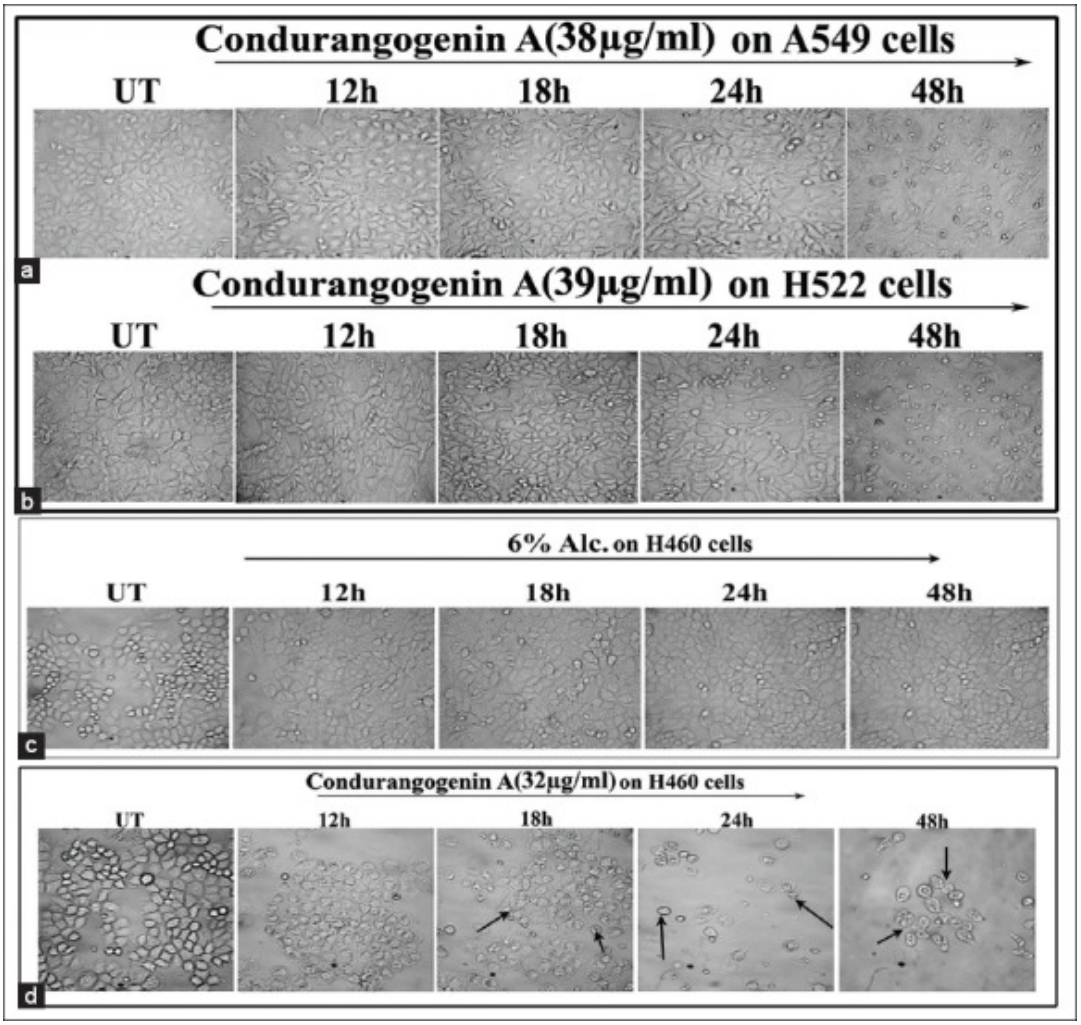

Open in a separate window

Analysis of cellular morphology by light microscopy (×40) (a) A549 cells were treated with condurangogenin A (ConA) (38 µg/ml) for 12 h, 18 h, 24 h and 48 h. Morphological changes were observed by phase contrast light microscope. Untreated denotes UT. (b) H522 cells were treated with ConA (39 µg/ml) for 12 h, 18 h, 24 h and 48 h. Morphological changes were observed by phase contrast light microscope. Untreated denotes UT. (c) H460 cells were treated with 6% Alc.(0.4 µl/ml) and (d) ConA (32 µg/ml) for 12 h, 18 h, 24 h and 48 h. Morphological changes were observed by phase contrast light microscope. Untreated denotes UT

Figure 5

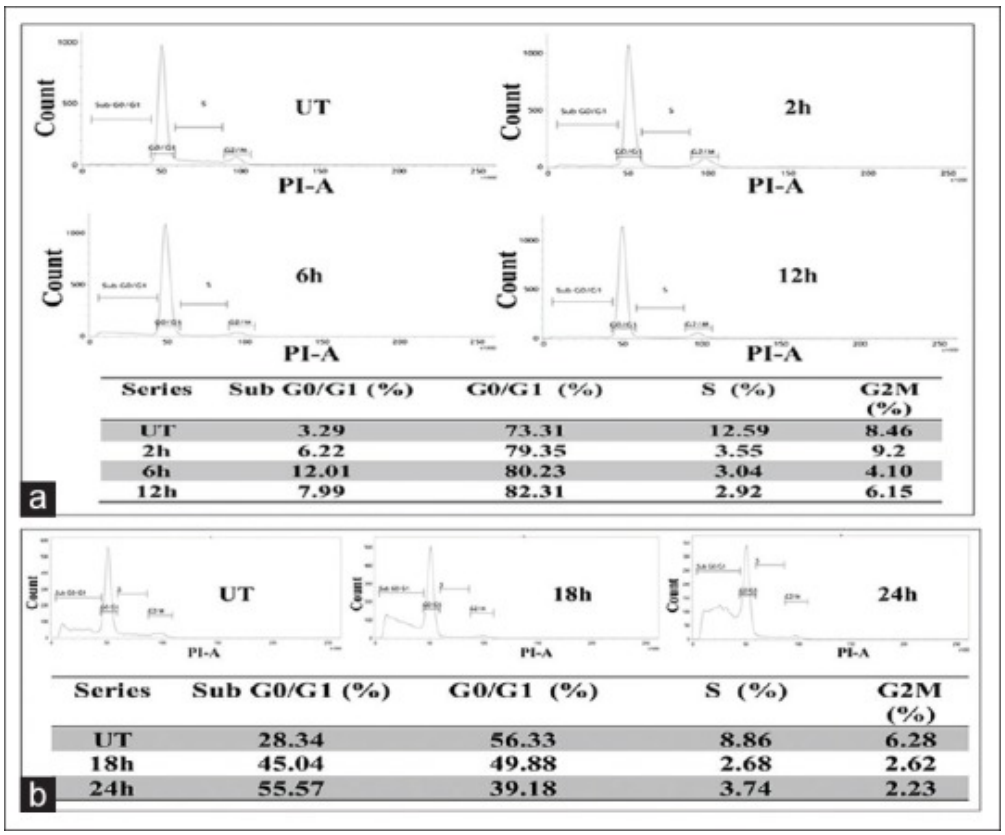

Analysis on cell cycle distribution (a) flow cytometric analysis of condurangogenin A (ConA)-treated H460 cells showed at early hours (2 h, 6 h, 12 h) of treatment (32 µg/ml dose), maximum cells were arrested at G0/G1 phase with the increase of time-points against untreated cells (UT). (b) For the long term of ConA treatment (18 h and 24 h), sub G0/G1 cell population was certainly increased gradually with the decrease of G0/G1, further indicate the presence of sub-diploid cell population which may trigger apoptosis for long-term effect of ConA treatment with respect to untreated cells

Figure 6

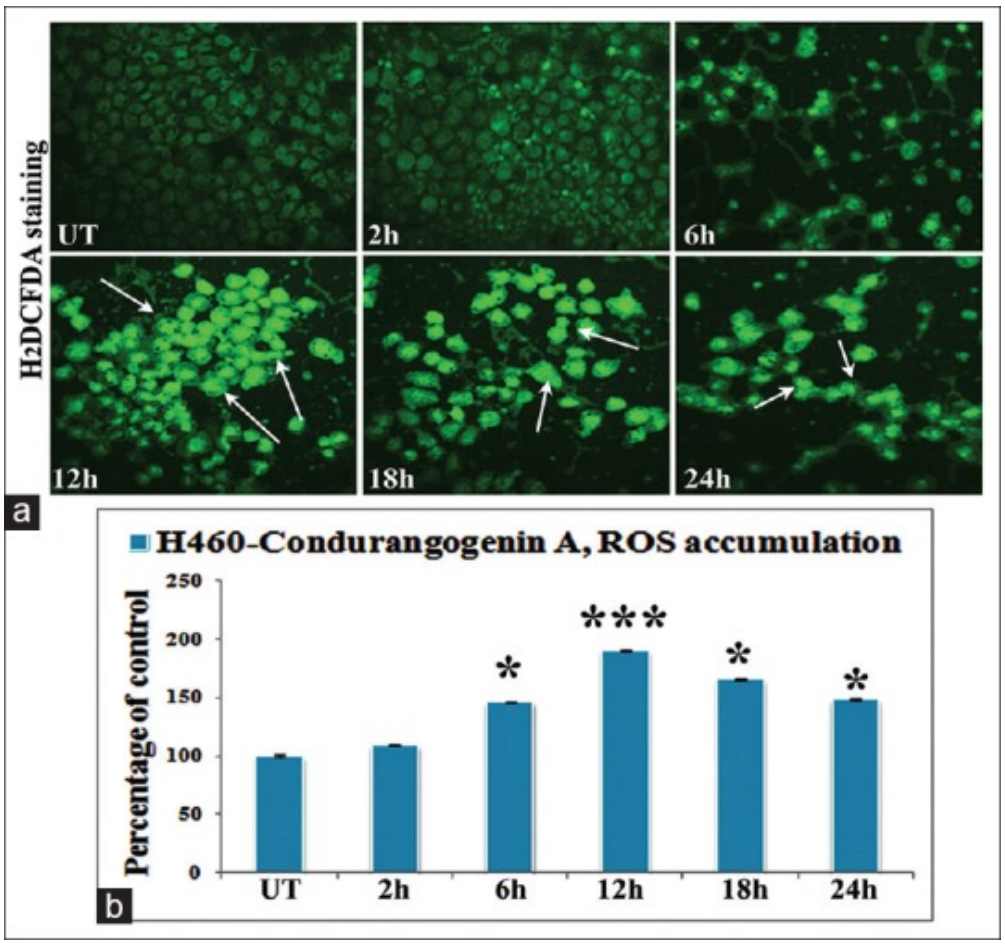

Open in a separate window

Intracellular reactive oxygen species (ROS) accumulation by fluorescence microscopic (×40) and fluorimetric study (a) figures showed very low fluorescence intensity (both qualitatively and quantitatively) in untreated cells (UT), while the maximum fluorescence intensity was observed at 12 h of condurangogenin A treatment. (b) The fluorimetric data revealed that at ROS accumulation was increased at 6 h, 12 h, 18 h and 24 h, but at 12 h time-point ROS accumulation was significantly maximum than UT. Significance, *$P < 0.05$ versus UT and ***$P < 0.001$ versus UT

Figure 7

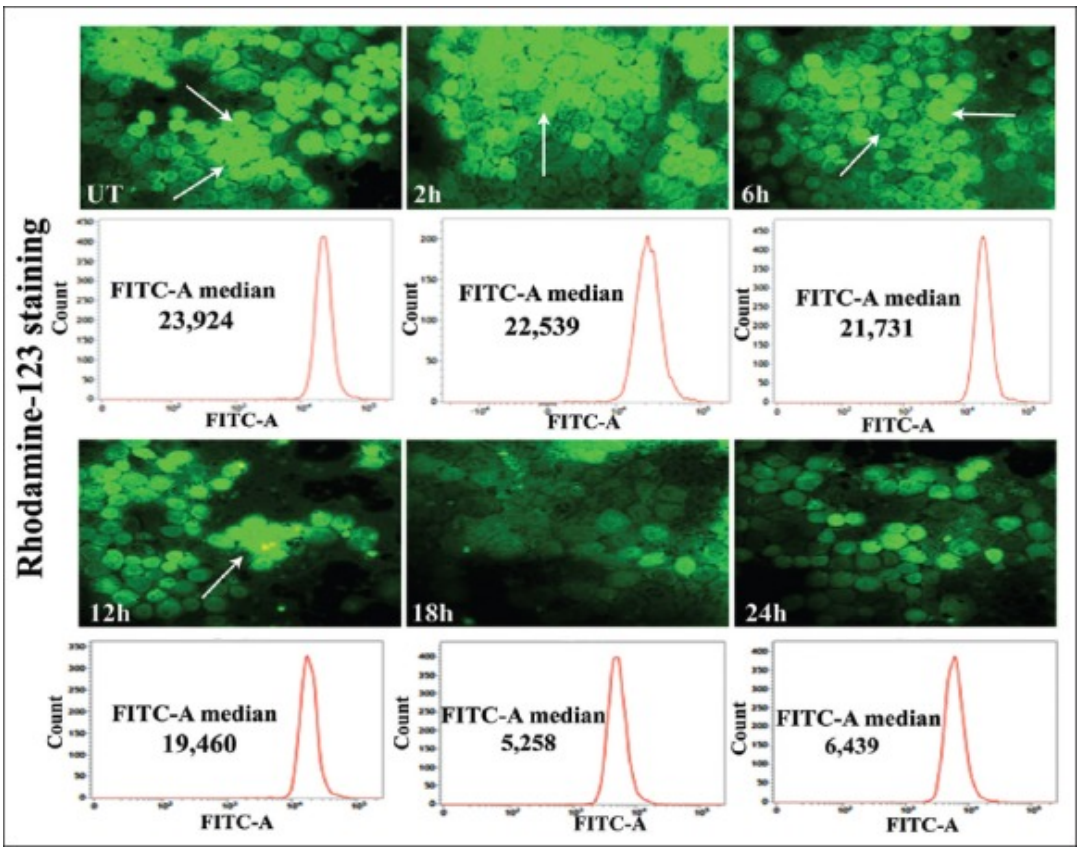

Open in a separate window

Analysis of the changes in mitochondrial membrane potential (MMP) results of rhodamine 123-staining indicated bright green fluorescence in untreated cells (UT), while the cells treated with condurangogenin A (32 µg/ml), showed gradual decrease of fluorescence intensity with the lapse of time (2, 6, 12, 18, 24 h), specifically at 18 h time-point which denote the loss of MMP (×40). The flowcytometric study also revealed that at 18 h time-point the FITC-A median of rhodamine 123 was very low (5, 258) than the UT (23, 924) and other time-points

Figure 8

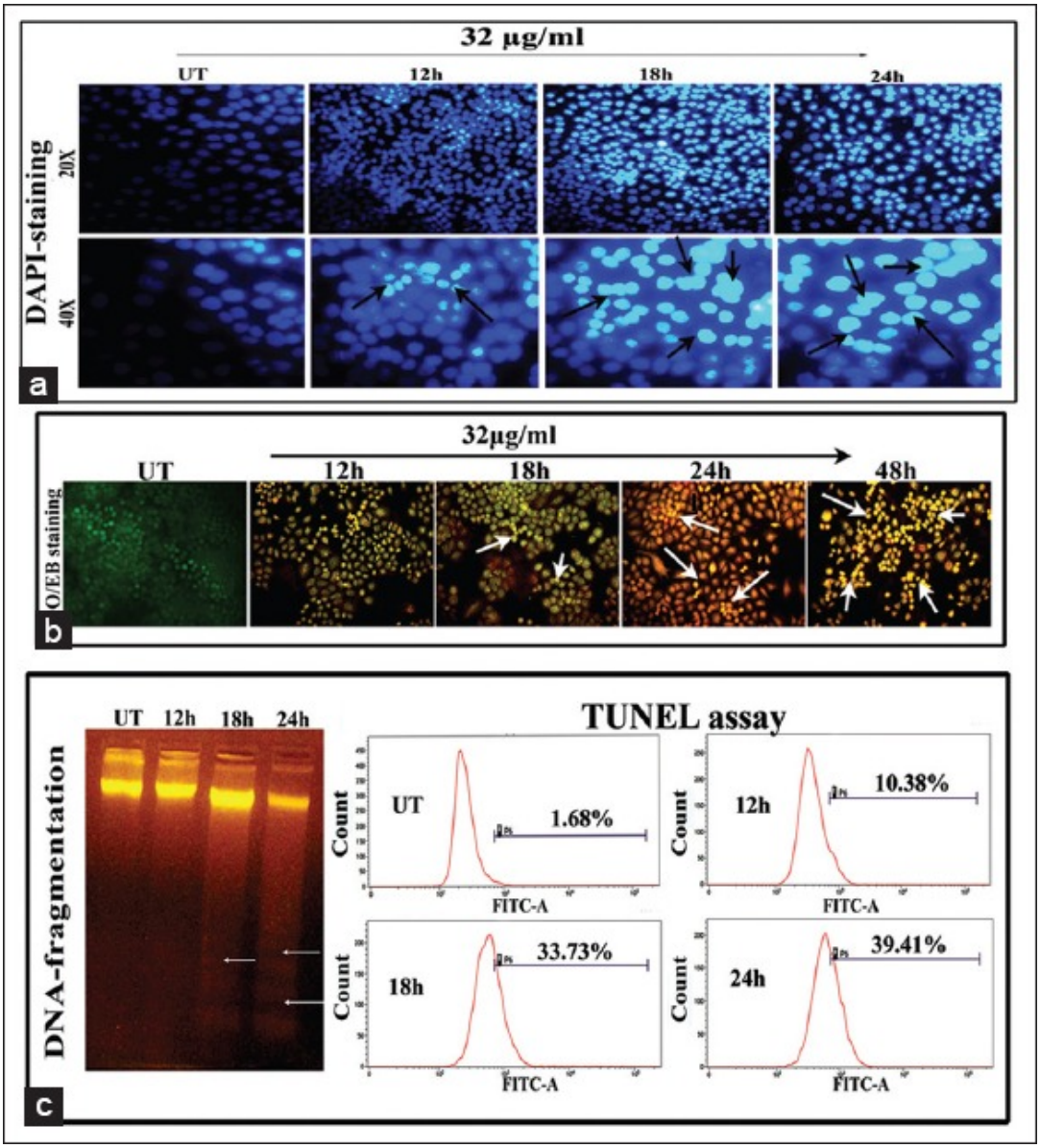

Open in a separate window

(a) Changes in nuclear morphology observed by diaminophenylindole (DAPI) staining (×20 and × 40). Figures represent the gradual increase of DAPI-fluorescence intensity due to increase of DNA nick with the increase of time-points of Con A treatment in H460 cells. The representative arrows denote the DNA nicks and nuclear deformities (b) acridine orange/ethidium bromide (AO/EB) dual-staining assay (×20). The gradual increase of the EB-florescence intensity was observed in Con A-treated cells, but remarkably observed at 24 h time-point, indicated the fragmentation of DNA (indicated by arrows). (C) DNA fragmentation assay represents the formation of DNA laddering (indicated with arrows) specifically at 18 h and more in 24 h time-point of Con A treatment in respect to UT due to DNA breakage which indicates apoptosis generation at late hours of Con A treatment. Deoxyuridine triphosphate end labelling by TUNEL assay. Figures showed the gradual increase of TUNEL-positive cells with increase of time of Con A treatment against UT and the maximum DNA breakage was observed at 24 h of treatment (39.41%)

Figure 9

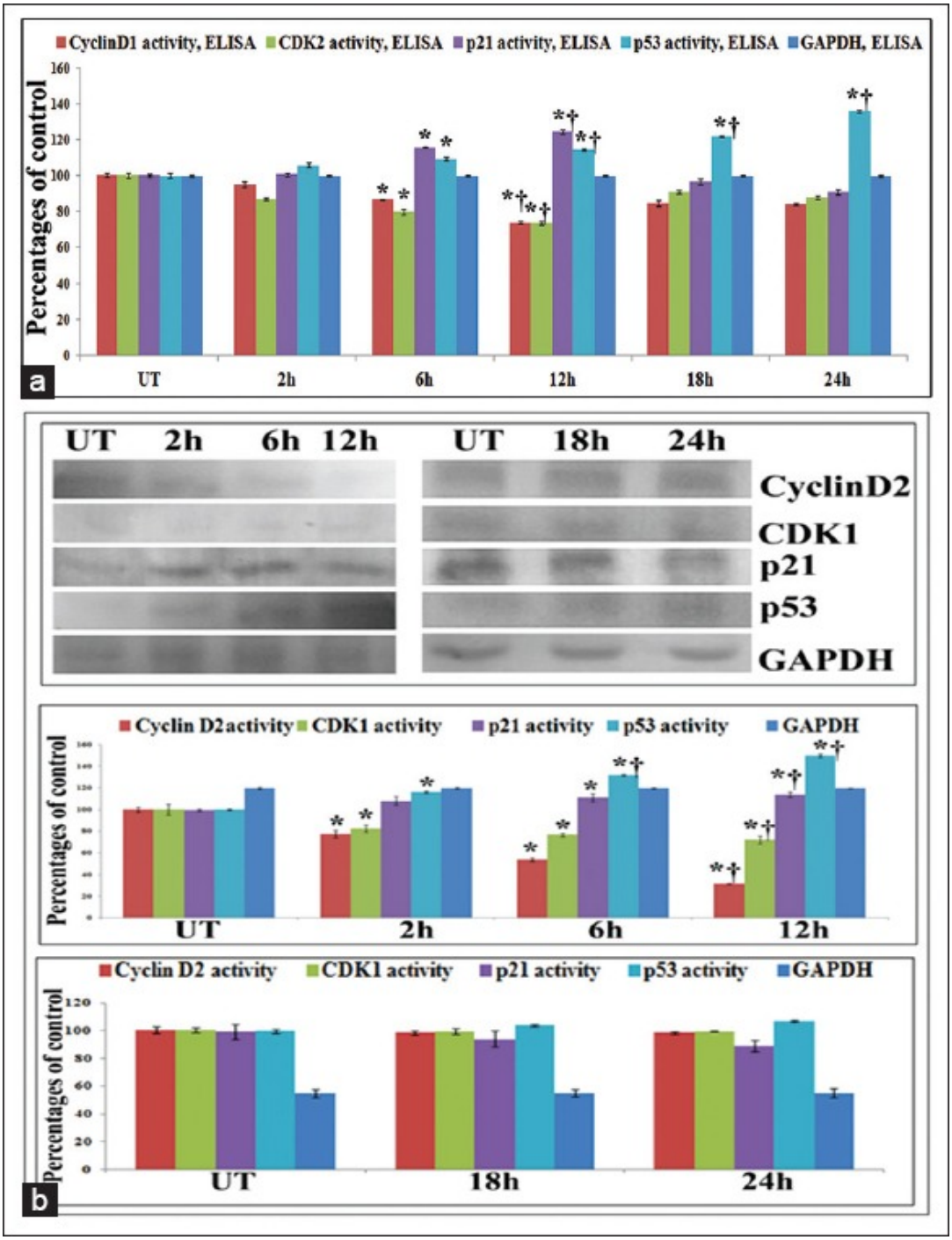

Open in a separate window

(a) Enzyme linked immunosorbent assay (ELISA) of cell cycle markers. Results of ELISA showed significant downregulation of cyclin D1-CDK2 with p21 and p53 up-regulation in the early phases (2 h, 6 h, 12 h) of Con A treatment (32 μg/ml), specifically at 12 h against untreated samples. But in the late phases of treatment (18 h and 24 h), downregulation of cyclin D1-CDK1 and p21 was found with the significant increased expression of p53 (b) Western blots of cell cycle markers. Results showed significant downregulation of cyclin D1-CDK2 with p21 and p53 up-regulation in the early phases (2 h, 6 h, 12 h) of Con A treatment (32 μg/ml), specifically at 12 h against untreated samples. But in the late phases of treatment (18 h and 24 h), downregulation of cyclin D1-CDK1 and p21 was found with the significant increased expression of p53. Results are expressed as mean ± standard deviation ($N = 6$). Significance, *$P < 0.05$ versus untreated (UT) and †$P < 0.001$ versus UT

Figure 10

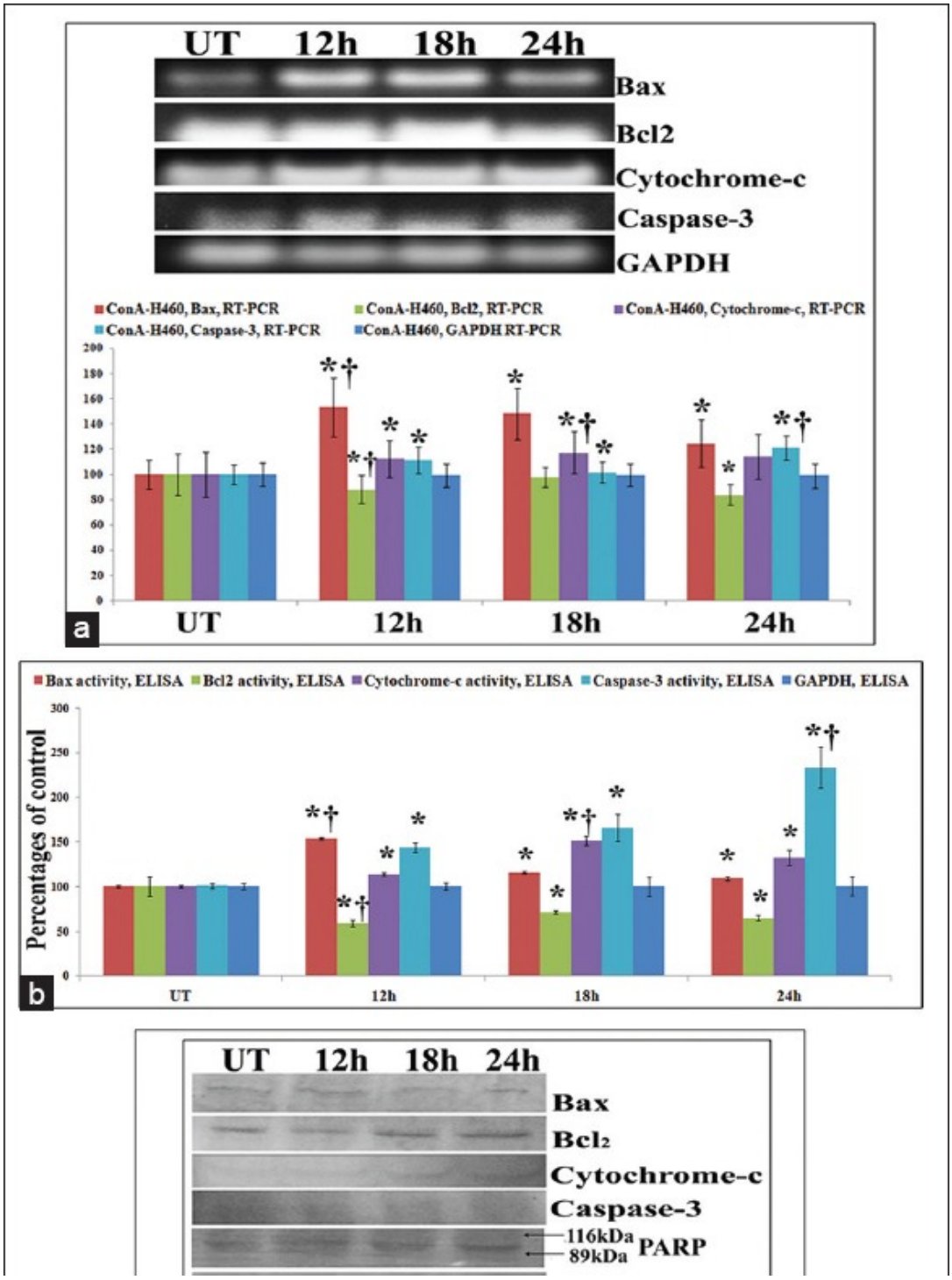

Open in a separate window

(a) Study on apoptosis markers at mRNA level by reverse transcriptase polymerase chain reaction (RT-PCR) and (b) at protein level by enzyme linked immunosorbent assay (ELISA). The results of RT-PCR and ELISA of Bax/Bcl2 revealed significant upregulation of Bax and downregulation of Bcl2 at 12 h of treatment against untreated samples. The results of cytochrome-c expression at mRNA and protein level revealed that at 18 h of treatment cytochrome-c expression was at the maximum as compared to the untreated control. Significant increase of expression of caspse-3 at 24 h interval was observed against UT that triggers apoptosis. Results are expressed as mean ± standard deviation (SD) ($N = 6$). Significance, *$P < 0.05$ versus untreated (UT) and †$P < 0.001$ versus UT. (c) Study on apoptosis markers at protein level by western blot. The results of Bax/Bcl2 revealed significant upregulation of Bax and downregulation of Bcl2 at 12 h of treatment against untreated samples. The results of cytochrome-c expression revealed that at 18 h of treatment

cytochrome-c expression was at the maximum as compared to the untreated control. Significant increase of expression of caspse-3 at 24 h interval was observed against UT that stimulates the cleavage of PARP. The western blot analysis of PARP at different hour intervals showed that at 24 h time-point, PARP cleavage occurred by the formation of active 89 kDa and inactive 116 kDa subunits where band-intensity was significantly increased in 89 kDa fragment against untreated controls. Results are expressed as mean ± SD ($N = 6$). Significance, *$P < 0.05$ versus untreated (UT) and †$P < 0.001$ versus UT

Figure 11

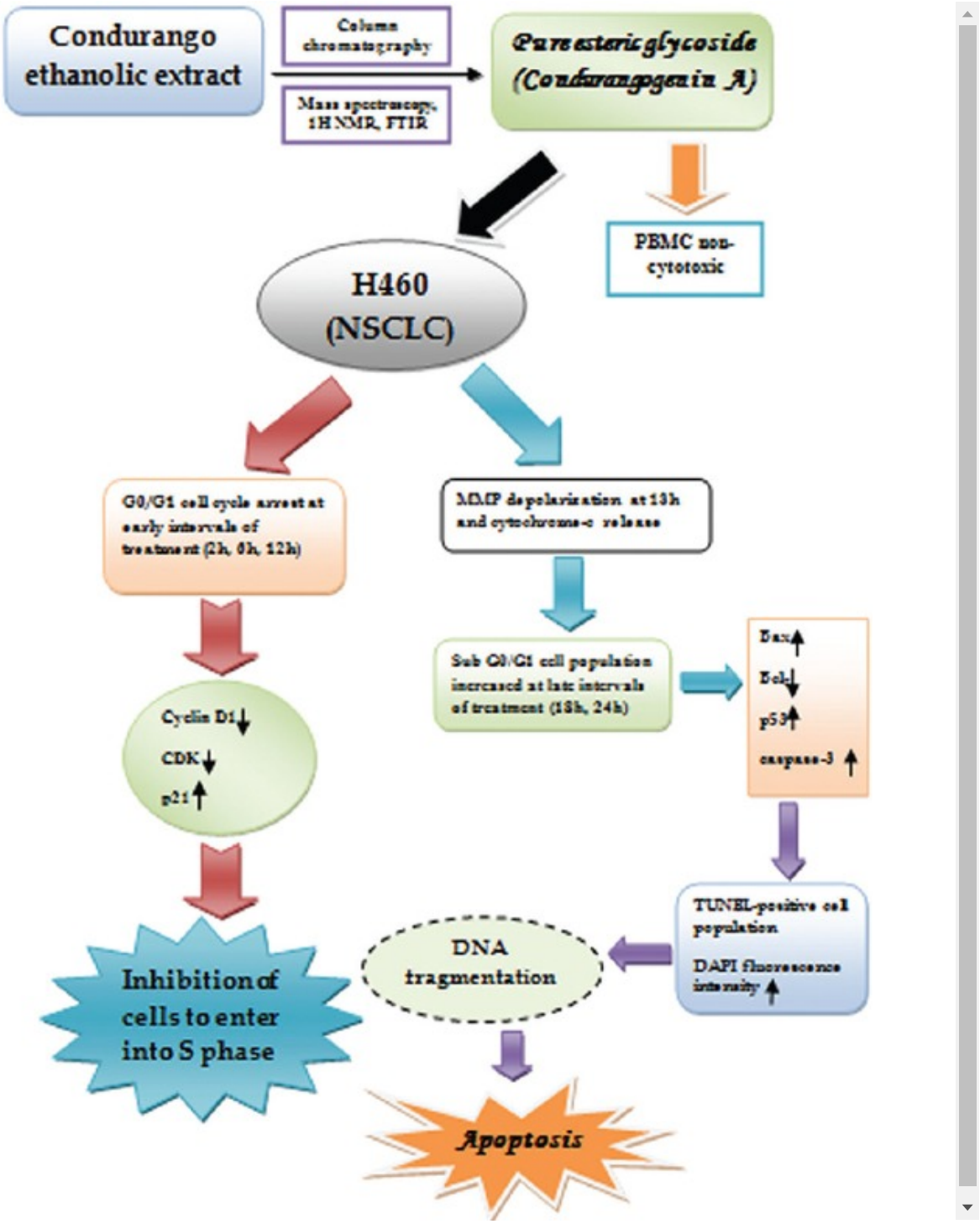

Open in a separate window

Simple schematic representation of effect of condurangogenin A (ConA) against nonsmall-cell lung cancer cells *in vitro* via p21/p53 mediated cell cycle modulation and DNA damage-induced apoptosis